Serum Tryptophan-Derived Quinolinate and Indole-3-Acetate Are Associated With Carotid Intima-Media Thickness and its Evolution in HIV-Infected Treated Adults

Anders Boyd,[1,*] Franck Boccara,[2,3,*] Jean-Luc Meynard,[4] Farid Ichou,[5] Jean-Philippe Bastard,[3,6] Soraya Fellahi,[3,6] Assia Samri,[7] Delphine Sauce,[7] Nabila Haddour,[2] Brigitte Autran,[7] Ariel Cohen,[2] Pierre-Marie Girard,[1,4] Jacqueline Capeau;[3] and the Collaboration in HIV, Inflammation and Cardiovascular Disease study

[1]Inserm UMR_S1136, Sorbonne Université, Institut Pierre Louis d'Epidémiologie et de Santé Publique (IPLESP), Paris, France, [2]Department of Cardiology, AP-HP, Hôpital Saint-Antoine, Paris, France, [3]Faculty of Medicine, Sorbonne Université, Inserm UMR_S938, ICAN, Paris, France, [4]Department of Infectious Diseases, APHP, Hôpital Saint-Antoine, Paris, France, [5]Institute of Cardiometabolism and Nutrition, ICAN, ICANalytics, Paris, France, [6]Department of Biochemistry, APHP, Hôpital Tenon, Paris, France, and [7]Sorbonne Université, INSERM U1135, Centre d'Immunologie et des Maladies Infectieuses, Paris, France

Background. HIV-infected individuals undergoing effective antiretroviral therapy (ART) present an increased risk of atherosclerotic cardiovascular disease. We identified serum metabolites associated with carotid intima-media thickness (c-IMT) and its evolution.

Methods. One hundred forty-three hydrophilic serum metabolites were measured by ultraperformance liquid chromatography coupled with high-resolution mass spectrometry in 49 HIV+ ART+, 48 HIV+ ART-naïve and 50 HIV-negative, age-matched, never-smoking male triads. Metabolites differentially altered between groups ("features") were defined as having a Benjamini-Hochberg-adjusted P value <.05 from a t test and >0.25 $\log_2$ absolute mean fold change in metabolite levels. c-IMT was measured across 12 sites at inclusion in all individuals and at the carotid artery (cca) after a median of 5.1 years in 32 HIV+ ART+ individuals. The difference in c-IMT (cross-sectional analysis) and slope of cca-IMT regression/progression per year (longitudinal analysis) for each $\log_{10}$ (area) increase in metabolite level were estimated with linear regression.

Results. Compared with HIV-, metabolite features of HIV+ ART+ were increased N6,N6,N6-trimethyl-L-lysine and decreased ferulate and 5-hydroxy-L-tryptophan, whereas features of HIV+ ART-naïve were increased malate, kynurenine, 2-oxoglutarate, and indole-3-acetate and decreased succinate and 5-hydroxy-L-tryptophan. In HIV+ ART+ individuals, quinolinate and/or indole-3-acetate were positively associated with c-IMT ($P < .03$), cca-IMT ($P < .03$), and cca-IMT progression ($P < .008$). These associations were not observed in HIV+ ART-naïve or HIV-negative individuals. In HIV+ ART+ individuals, the metabolites xanthosine and uridine, from nucleotide metabolism, and g-butyrobetaine, from lysine/dietary choline degradation, were also positively or negatively associated with c-IMT and/or cca-IMT (all $P < .01$), but not its evolution.

Conclusions. In these highly selected HIV-positive ART-controlled males, 2 novel metabolites derived from tryptophan catabolism, indole-3-acetate and quinolinate, were associated with c-IMT and its progression.

Keywords. antiretroviral; cardiovascular disease; carotid intima-media thickness; HIV; metabolomics; tryptophan metabolism.

Cardiovascular disease (CVD) has become a major concern in HIV-positive individuals, even for those with well-controlled HIV replication during antiretroviral therapy (ART) [1, 2].

Increases in atherosclerotic cardiovascular risk have been reported for HIV-positive individuals, whether based on cardiovascular outcomes or carotid intima-medial thickness (c-IMT), a validated surrogate marker of atherosclerotic vascular disease [3]. Prior studies have linked host factors, such as smoking and illicit drug use, and HIV-related factors, such as known infection duration [4], immune activation [5], and treatment with protease inhibitors [6, 7], to this increased risk. Nevertheless, the precise pathophysiological mechanisms remain uncertain to date.

Metabolomics, able to identify numerous circulating metabolites, could provide important information on the processes involved in atherosclerotic cardiovascular risk. Such analyses have been used in past research, in which metabolite levels were

associated with HIV serostatus, severity of HIV infection, low-grade inflammation in HIV-positive individuals with virological suppression, and long-term non-AIDS-related events [8]. Most previous research has focused on the tryptophan (Trp) catabolic pathway and kynurenine/tryptophan ratio (KTR), resulting from indoleamine-pyrrole 2,3-dioxygenase (IDO) activation [9–12], and trimethylamine (TMA) and trimethylamineoxide (TMAO) of the lysine/dietary choline degradation pathway [13, 14].

Notwithstanding the insights gained from these previous studies, their major limitation is that only specific metabolites of distinct pathways were analyzed. To understand the broader scope of potentially involved metabolites, we analyzed 143 hydrophilic metabolites, including all amino acids and metabolic derivatives, and their association with HIV infection and c-IMT. Using data from a previous study in closely matched, never-smoking male adults who were HIV-positive ART-controlled, HIV-positive ART-naïve, or HIV-negative, we took advantage of the minimal confounding bias offered from these triads to evaluate the effect of HIV infection and treatment on metabolite levels. We then focused on HIV-positive ART-treated patients to establish the relationship between metabolite levels and c-IMT. Their correlation with markers of inflammation and HIV infection severity was also assessed.

METHODS

Study Participants and Samples
Participants were selected from the Collaboration on HIV, Inflammation and Cardiovascular disease (ANRS-CHIC) study [4]. Briefly, 150 never-smoker men were enrolled in 3 groups: 50 HIV-1-infected patients >35 years old, taking ART for ≥4 years, and with HIV-1 RNA <400 copies/mL (HIV+ ART+); 50 individually age-matched (±5 years) patients, HIV-positive for ≥2 years, who were naïve to ART (HIV+ ART-); and 50 HIV-negative patients individually age-matched (±5 years) to the index HIV-positive, treated patient (HIV-). Noninclusion criteria were current/former smokers; history of coronary heart disease, stroke, angina, or myocardial infarction; active/chronic viral hepatitis infection; undergoing systemic chemotherapy or steroids. All participants gave their written informed consent, and the protocol was approved by the Hotel-Dieu Ethics Committee.

For this study, we included participants with available serum samples. Individuals with severe renal dysfunction (estimated creatinine clearance <30 mL/min) were excluded due to the strong effect of kidney function on metabolite concentrations [15].

Carotid Intima-Media Thickness Measurements
c-IMT was calculated as a composite measure (12-site mean) of the maximal common carotid artery (cca)–IMT, bifurcation IMT, and internal carotid artery IMT bilaterally, outside of plaque, and are reported in mm [4]. c-IMT measurements were performed offline with quality IMT automatic measurement software. A subgroup of patients in the HIV+ ART+ group also had a second measurement of cca-IMT a median (interquartile range) of 5.1 (4.8–5.3) years from participating in the cross-sectional study.

Laboratory Measurements
Individuals had been fasting (12 hours) before their visit. Blood samples were retrieved and processed at a single center and stored at –80°C until use. Interleukin (IL)-6, IL-10 (Bender Medsystems, Burlingame, CA, USA), resistin, and soluble(s) CD14 (R&D Systems, Minneapolis, MN, USA) levels were analyzed using an enzyme-linked immunosorbent assay. Serum ultrasensitive C-reactive protein (us-CRP) was measured by immononephelometry on an IMMAGE analyzer (Beckman-Coulter, Miami, FL, USA). Plasma D-dimer was measured by enzyme-linked fluorescent assay on a VIDAS analyzer (Biomérieux, Marcy-l'Etoile, France). Inducible protein (IP)–10, fractalkine, Monokine induced by gamma interferon (MIG), monocyte chemoattractant protein (MCP)–1, E-selectin, and tumor necrosis factor (TNF)–α were quantified from plasma using the BD Cytometric Bead Array system (BD, Franklin Lakes, NJ, USA).

Immunological Function
Cell samples were available on a randomly selected subset of 30 HIV+ ART+ patients [16]. Activated CD8+ and CD4+ memory T cells (CCR7-CD27-CD45RA+/-, defined by expression of the CD38 and Ki67 markers) and immunosenescence (defined by expression of CD57 on memory T cells) were analyzed on a LSR2 flow cytometer (Becton Dickinson, Franklin Lakes, NJ, USA) with appropriate isotype controls and color compensation.

Ultraperformance Liquid Chromatography Coupled With High-Resolution Mass Spectrometry Metabolomics
Reference compounds and a 13C and 15N stable isotope-labeled mix of amino acids were purchased from Sigma-Aldrich (Saint Quentin Fallavier, France), along with liquid chromatography–mass spectrometry (LC-MS)–grade solvents, acetonitrile, and formic acid. Deionized water was obtained from a Milli-Q Elix system fitted with a LC-PaK and a MilliPak filter at 0.22 µm (Merck Millipore, Guyancourt, France).

Sample preparation and liquid chromatography coupled with high-resolution mass spectrometer experiments were carried out as reported [17, 18]. Briefly, 8 volumes of frozen acetonitrile (–20°C) containing internal standard (labeled mixture of amino acids at 12.5 µg/mL) were added to 100 µL of serum samples and vortexed. The resulting samples were then sonicated and incubated at 4°C during 1 hour for slow protein precipitation. Samples were centrifuged for 20 minutes at 20.000×g at 4°C. Supernatants were transferred to another series of tubes and

then dried and stored at –80°C before LC-MS analyses. Samples were reconstituted in a 3-fold dilution of H2O/ACN (95/05).

Ultraperformance liquid chromatography coupled with high-resolution mass spectrometry experiments were performed using a chromatographic column Discovery HS F5-PFPP, 5 μm, 2.1×150 mm (Sigma, Saint Quentin Fallavier, France) at 35°C in a UPLC Waters Acquity (Waters Corp, Saint-Quentin-en-Yvelines, France) and Q-Exactive mass spectrometer (Thermo Fisher Scientific, Illkirch, France).

Statistical Analysis

To perform our analysis, we used pathways of the major mapped metabolites from the Kyoto Encyclopedia of Genes and Genomes (KEGG) [19] that have been involved in previous studies on HIV/ART or c-IMT. These metabolic pathways were purine and pyrimidine metabolism, lysine and dietary choline catabolism, tryptophan catabolism, and citrate cycle. All metabolite levels are reported in $\log_{10}$-transformed area values ($\log_{10}$ (area)).

In an initial analysis, we examined metabolite differences between HIV/ART groups. First, we compared the overall variation of metabolite levels, within the 4 selected pathways, across groups using an *F*-statistic from Wilks' lambda in a multivariate analysis of variance (MANOVA). Second, we identified metabolite features that were differentially altered between HIV/ART groups. Mean metabolite levels were compared between (i) HIV+ ART+ vs HIV-, (ii) HIV+ ART- vs HIV-, and (iii) HIV+ ART+ vs HIV+ ART- using an unpaired *t* test. *P* values were adjusted using the Benjamini-Hochberg procedure. The $\log_2$ mean fold change of the $\log_{10}$ (area) levels between groups was also calculated for each metabolite. We defined metabolite features as those with an adjusted *P* value <.05 and a >.25 or <−.25 $\log_2$ mean fold change in $\log_{10}$ (area). This analysis was carried out using the R package "omu."

In a subsequent analysis, we focused on HIV+ ART+ participants and studied the relationship between metabolite levels and c-IMT. We first used univariable analyses to identify candidate metabolites, which were tested in subsequent analyses. First, change in c-IMT for each $\log_{10}$ (area) increase in metabolite level was estimated with linear regression in univariable analysis. A multivariable analysis model was constructed in which an a priori selection of covariables based on prior research [4, 15] (age, prior hypertension, diabetes, and creatinine clearance) and metabolites with *P* < .1 in univariable analysis were included, whereas metabolites with *P* > .1 were removed in backwards-stepwise fashion. Second, the same metabolites associated with c-IMT in univariable analysis were used to model (1) change in cca-IMT for each $\log_{10}$ (area) increase in metabolite level and (2) change in slope of cca-IMT regression/progression per year for each $\log_{10}$ (area) increase in metabolite concentration among those with 2 cca-IMT measurements. Univariable and multivariable models were constructed as above. Significance for these analyses was determined by a *P*

value <.05, and no *P* value adjustments were made in order to avoid adverse reduction in type II error [20].

Other analyses were conducted to determine the correlation (Spearman rank) between metabolites of the same pathway, as illustrated with correlation networks using Cytoscape, version 3.6.1 [21], and to determine the correlation between metabolites and markers of inflammation/immunity or HIV severity, as illustrated with heatmaps using the R package "gplots." Significance for these analyses was determined by a *P* value <.05.

Statistical analysis was performed using STATA (version 12.1; College Station, TX, USA) and R (version 3.2.0; Vienna, Austria).

RESULTS

Characteristics of the Study Population

Of the 150 included males, 2 without an available serum sample and 1 with severe renal dysfunction in the HIV+ group were not included.

Demographic, HIV-related, and cardiovascular-related characteristics are described in Supplementary Table 1. The large majority had a BMI <30 kg/m^2 (97%), and only 6% had ≥1 comorbidity (diabetes, prior hypertension, or moderate renal dysfunction). Any use of cannabis, cocaine, and/or methamphetamine within <12 months was most common in HIV+ ART+ participants (28.6%), followed by HIV+ ART- (12.5%) and HIV- (2.0%) participants (*P* < .001). In the HIV+ ART+ group, HIV-infection was mostly controlled, with a median ART duration >4 years and 94% under viral suppression (<50 copies/mL).

Differences in Metabolites Between HIV/ART Groups

Using MANOVA, significant variations in metabolite levels were observed in the tryptophan metabolism (*P* < .001) and citrate cycle (*P* < .001) pathways, but not purine/pyrimidine metabolism (*P* = .08) or lysine and dietary choline catabolism (*P* = .14). Metabolite features were as follows: HIV+ ART+ vs HIV-: increased relative levels of N6,N6,N6-trimethyl-L-lysine and decreased ferulate and 5-hydroxy-L-tryptophan (Figure 1A); HIV+ ART- vs HIV-: increased malate, kynurenine, 2-oxoglutarate, and indole-3-acetate and decreased succinate and 5-hydroxy-L-tryptophan (Figure 1B); and HIV+ ART+ vs HIV+ ART-: decreased succinate (Figure 1C).

Correlation Between Metabolites of the Same Pathway According to HIV/ART Groups

In the purine/pyrimidine metabolism pathway (Figure 2A), a strong correlation was observed between inosine and guanosine in HIV+ ART+ individuals (*rho* = .836; *P* < .001), which remained in HIV- individuals (Supplementary Figure 1A). In the lysine and dietary choline catabolism pathway (Figure 2B), strong correlations were observed between pipecolate and carnitine (*rho* = .408; *P* = .004), N6,N6,N6-trimethyl-L-lysine
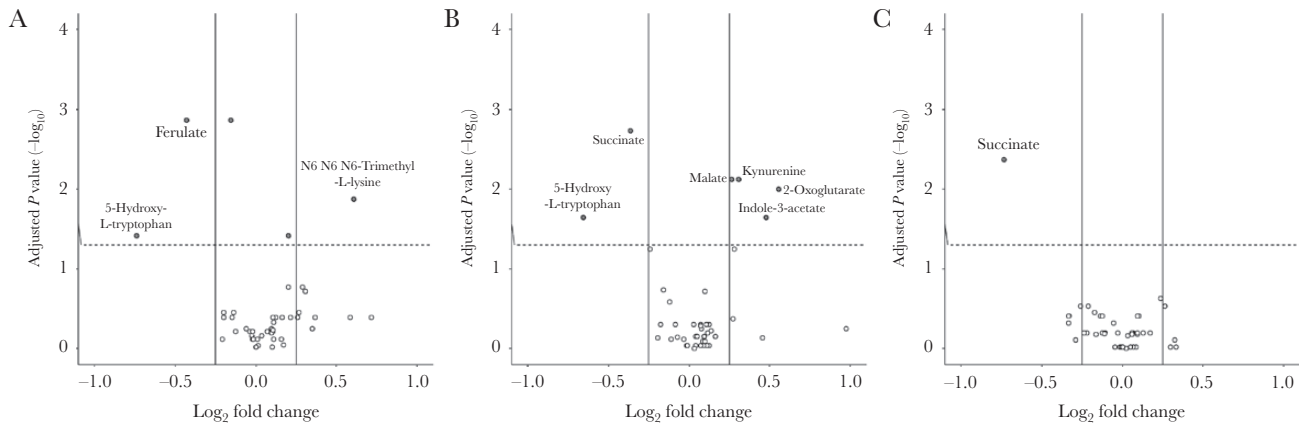
Figure 1. Metabolite features of the HIV and antiretroviral therapy (ART) groups. Adjusted P values ($-\log_{10}$) from a t test comparing mean metabolite levels in $\log_{10}$ (area) between groups are plotted against their relative $\log_2$ mean fold change. Each dot represents a metabolite; metabolite names are only given for those fulfilling criteria as a metabolite feature: adjusted P value <.05 and $\log_2$ mean fold change >0.25 or <−0.25. Comparisons are between: HIV+ ART+ vs HIV- (A), HIV+ ART- vs HIV- (B), and HIV+ ART+ vs HIV+ ART- (C).
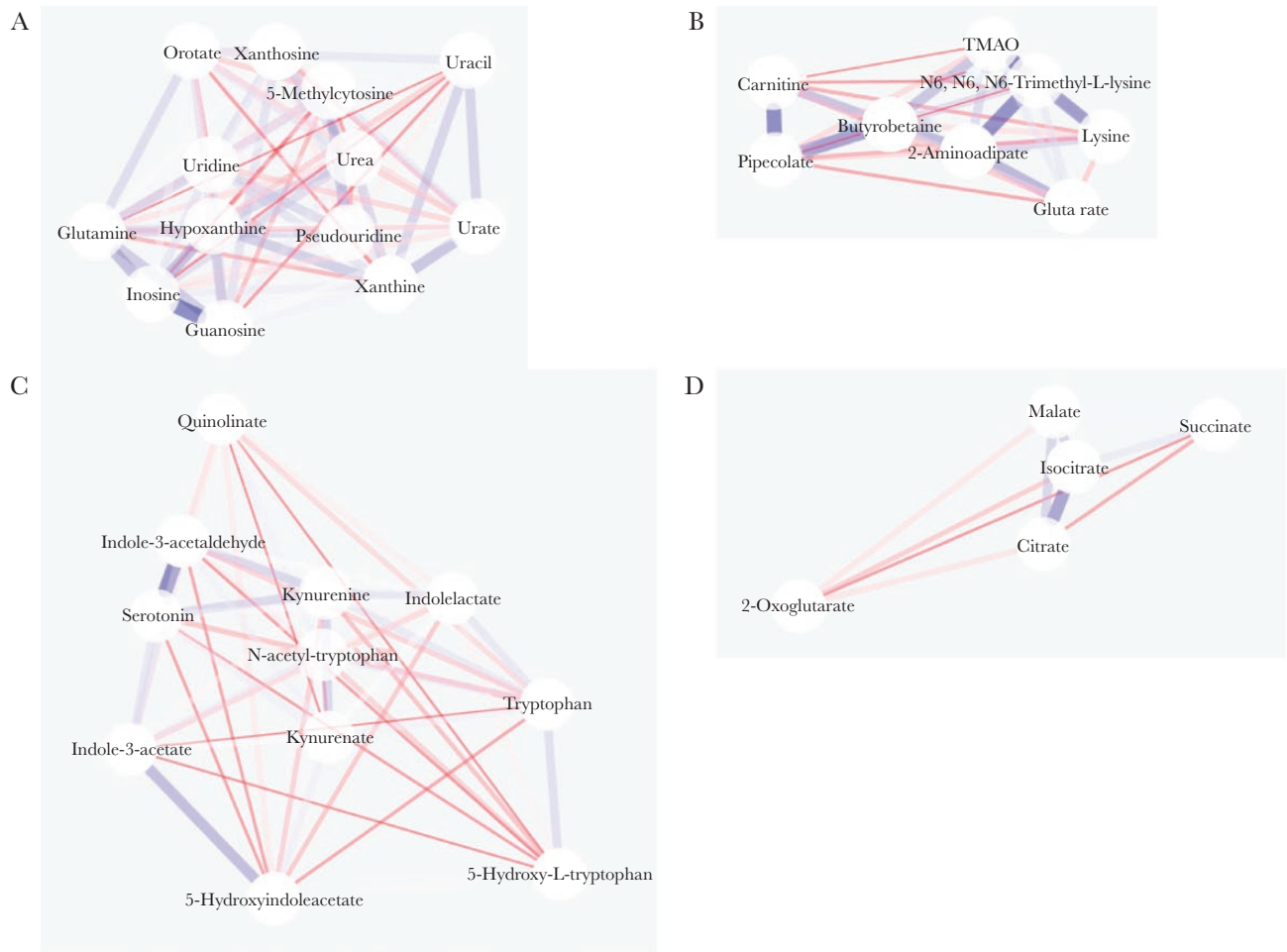

Figure 2. Correlation networks between metabolites in HIV-positive patients treated with antiretroviral therapy. Correlation networks between metabolites of the purine/pyrimidine metabolism (A), lysine degradation (B), tryptophan metabolism (C), and citrate cycle (D) pathways. Positive and negative correlations are depicted in blue and red, respectively. Stronger correlations have thicker lines and colored shading. Metabolites are arranged in an edge-weighted, spring-embedded layout.

Table 1. Metabolites Associated With Carotid Intima-Media Thickness and Common Carotid Artery–IMT in HIV-Positive Patients Treated With Antiretroviral Therapy

	Univariable[a]		Multivariable[b]	
Total c-IMT Cross-sectional[c] (n = 49)	Diff (95% CI), mm	P	Diff (95% CI), mm	P
Purine/pyrimidine metabolism				
Xanthosine	0.160 (0.005 to 0.314)	.04	0.128 (0.040 to 0.216)	.005
Uridine	0.283 (0.069 to 0.497)	.01	0.165 (0.041 to 0.289)	.01
Lysine degradation				
Pipecolate	−0.234 (−0.337 to −0.130)	<.001		
g-butyrobetaine	−0.344 (−0.577 to −0.110)	.004	−0.190 (−0.314 to −0.067)	.003
Tryptophan metabolism				
Indole-3-acetate	0.102 (0.009 to 0.194)	.03	0.056 (0.007 to 0.106)	.03
Quinolinate	0.169 (0.011 to 0.327)	.04	0.115 (0.018 to 0.211)	.02
cca-IMT cross-sectional[c] (n = 49)	Diff (95% CI), mm	P	Diff (95% CI), mm	P
Purine/pyrimidine metabolism				
Xanthosine	0.108 (−0.032 to 0.248)	.13		
Uridine	0.218 (0.024 to 0.413)	.03		
Lysine degradation				
Pipecolate	−0.193 (−0.288 to −0.099)	<.001		
g-butyrobetaine	−0.293 (−0.504 to −0.082)	.007	−0.227 (−0.399 to −0.054)	.01
Tryptophan metabolism				
Indole-3-acetate	0.118 (0.035 to 0.201)	.006	0.078 (0.010 to 0.145)	.03
Quinolinate	0.099 (−0.046 to 0.243)	.18		
cca-IMT progression[d] (n = 31)	Diff (95% CI), mm Δ/y	P	Diff (95% CI), mm Δ/y	P
Purine/pyrimidine metabolism				
Xanthosine	0.062 (−0.161 to 0.285)	.6		
Uridine	0.235 (−0.098 to 0.569)	.16		
Lysine degradation				
Pipecolate	−0.105 (−0.307 to 0.098)	.3		
g-butyrobetaine	−0.189 (−0.560 to 0.183)	.3		
Tryptophan metabolism				
Indole-3-acetate	0.148 (0.014 to 0.282)	.03	0.182 (0.053 to 0.311)	.008
Quinolinate	0.341 (0.083 to 0.599)	.01	0.400 (0.149 to 0.651)	.003

Data were obtained from HIV-infected patients treated with antiretroviral therapy.

Abbreviations: Δ, change; c-IMT, carotid intima-media thickness; cca, common carotid artery; diff, difference.

[a]Only metabolites with P values <.1 in univariable analysis (for the c-IMT cross-sectional analysis) are provided; all other estimates are provided in Supplementary Table 2. The metabolites in the c-IMT cross-sectional univariable analysis were used as candidates for the cca-IMT cross-sectional and progression analysis.

[b]Multivariable models were adjusted for age, hypertension, diabetes, and creatinine clearance. The following metabolites were excluded: c-IMT cross-sectional—pipecolate (P = .899); cca-IMT cross-sectional—uridine (P = .131), pipecolate (P = .432); cca-IMT progression—none.

[c]An evaluation of metabolite levels and c-IMT/cca-IMT was performed at the same moment in the cross-sectional studies. "Diff" represents the mm change in IMT for each log$_{10}$ (area) increase in metabolite level.

[d]In a subset of patients with a second cca-IMT measure (occurring a median [interquartile range] of 5.1 [4.8–5.3] years) after the first measure), metabolite levels at the time of first IMT measure were used to model mm change in cca-IMT per year. "Diff in mm Δ/y" represents the mm change in slope of IMT regression/progression for each log$_{10}$ (area) increase in metabolite level.

and lysine (*rho* = .322; *P* = .02), and N6,N6,N6-trimethyl-L-lysine and 2-aminoadipate (*rho* = .391; *P* = .005) in HIV+ ART+ individuals, whereas these correlations were not apparent in HIV- individuals (Supplementary Figure 1B). In the tryptophan metabolism pathway (Figure 2C), fairly weak correlations were observed between metabolites in HIV+ ART+ individuals, with the exception of indole-3-acetaldehyde and serotonin (*rho* = .989; *P* < .001), and while this correlation held in HIV- individuals (Supplementary Figure 1C), other correlations emerged. In the citrate cycle pathway (Figure 2D), only citrate and isocitrate were significantly correlated (*rho* = .439; *P* = .002), whereas this correlation and 1 between malate and isocitrate emerged in HIV- individuals (Supplementary Figure 1D).

Metabolites Associated With IMT and its Progression

Focusing on HIV+ ART+ individuals, we identified 4 metabolites associated with higher c-IMT levels (xanthosine, uridine, indole-3-acetate, and quinolinate) and 2 with lower c-IMT (pipecolate and g-butyrobetaine) in univariable analysis (Table 1). All except pipecolate remained significant in multivariable analysis, with additional adjustment for age, prior hypertension, diabetes, and creatinine clearance. Metabolites that were not associated with c-IMT in univariable analysis are presented in Supplementary Table 2.

We used the metabolites associated with c-IMT in univariable analysis as candidates for 2 subsequent multivariable analyses. First, cca-IMT was used as an end point and was found to be significantly associated with only g-butyrobetaine and indole-3-acetate (Table 1). Second, when examining the evolution of cca-IMT in the subset of participants with 2 measures, significantly faster progression of IMT was observed with higher baseline indole-3-acetate and quinolinate levels.

Of note, these associations were not observed in HIV+ ART-naïve (data not shown) or HIV-negative participants (Supplementary Table 3).

Metabolites Associated With Immune and Inflammatory Markers

Of the metabolites associated with c-IMT levels, most were not associated with profiles of high inflammation levels (Figure 3). However, uridine of the purine/pyrimidine metabolism pathway was strongly correlated with several markers of inflammation and cytokines (Figure 3A), and there was a significant correlation between quinolinate of the tryptophan metabolism pathway and TNF-α levels (*rho* = .334; *P* = .02) (Figure 3C). Of all the candidate metabolites, g-butyrobetaine was significantly correlated with percentage of naïve CD4+CD27+CD45RA+ (*rho* = .409; *P* = .03), memory CD4+ (*rho* = −.469; *P* = .009), naïve CD8+CD27+CD45RA+ (*rho* = .469; *P* = .009), and memory CD8+CD57+ senescent cells (*rho* = .422; *P* = .02) (Supplementary Figure 2). Pipecolate was also significantly correlated with percentage of CD4+CD57+ cells (*rho* = .378; *P* = .04).

Of note, 4 of the 5 metabolites involved in the citrate cycle were significantly associated with TNF-α and/or D-dimer (Figure 3D).
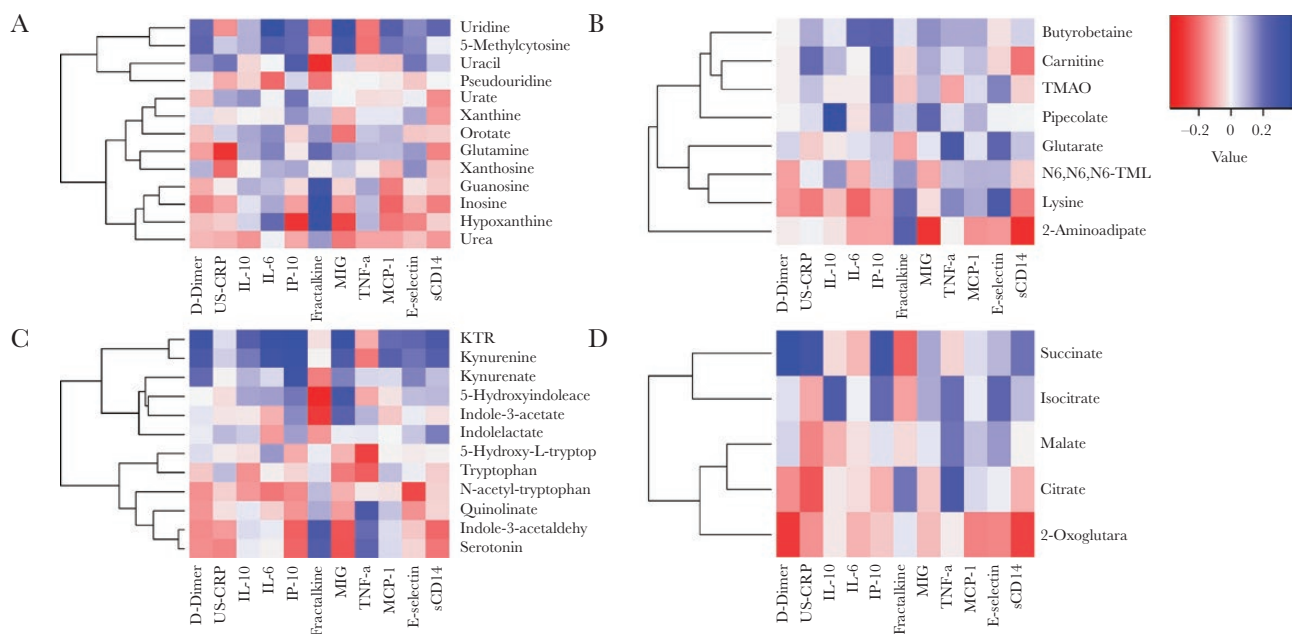

Figure 3. Correlation between metabolites and inflammatory markers in HIV-positive patients treated with antiretroviral therapy. Spearman correlations between metabolites and inflammatory markers are depicted in heatmaps for metabolites involved in purine/pyrimidine metabolism (A), lysine degradation (B), tryptophan metabolism (C), and the citrate cycle (D). Abbreviations: IL, interleukin; IP, inducible protein; MCP, monocyte chemoattractant protein; MIG, Monokine induced by gamma interferon; TMAO, trimethylamineoxide; TNF, tumor necrosis factor; US-CRP, ultrasensitive C-reactive protein.

Table 2.   Association Between Metabolites and Immunological Parameters in HIV-Positive Patients Treated With Antiretroviral Therapy

	Correlation		
	CD4+ T Cell	CD4+ Nadir	CD4:CD8 Ratio
Purine/pyrimidine metabolism			
Xanthine	–0.0486	**–0.2876**	–0.0912
Xanthosine	0.1053	0.1359	0.2084
Orotate	0.0398	**0.2889**	–0.0345
Uridine	0.1494	0.1091	0.2433
Lysine degradation			
Pipecolate	0.0510	0.0304	–0.0441
g-butyrobetaine	0.0844	0.0541	–0.0733
Carnitine	0.0848	**0.2886**	0.2886
Tryptophan metabolism			
Indole-3-acetate	0.0310	0.0310	0.0310
Kynurenate	**–0.2970**	–0.0900	–0.0647
Indolelactate	–0.1000	–0.0814	**–0.3054**
Quinolinate	0.0992	–0.0200	0.0825

Only metabolites with significant Spearman's correlations (as well as metabolites identified in the c-IMT cross-sectional analysis of Table 1) are provided; those with nonsignificant correlations are provided in Supplementary Table 4. Significant correlations are in bold.

Metabolites Associated With Markers of HIV Infection Severity

As shown in Table 2, none of the metabolites associated with c-IMT in univariable analysis were significantly correlated with CD4+ T-cell count, nadir CD4+, or CD4:CD8 ratio in HIV+ ART+ participants. Nevertheless, higher levels of xanthine were significantly correlated with lower CD4+ nadir, and higher orotate and L-carnitine levels with higher CD4+ nadir (Table 2). Higher indolelactate levels were significantly correlated with a lower CD4:CD8 ratio and kynurenate with lower CD4+ T-cell count. All other correlations are provided in Supplementary Table 4.

DISCUSSION

We report that in ART-controlled HIV-positive males but not HIV-positive ART-naïve or HIV-negative controls, c-IMT and its progression were positively associated with metabolites derived from the Trp catabolism pathway, indole-3-acetate and quinolinate. Xanthosine and uridine metabolites derived from purine/pyrimidine metabolism were positively associated with c-IMT, whereas the derivative g-butyrobetaine from the lysine and dietary choline degradation was inversely associated with c-IMT.

Of all the pathways studied, metabolites of Trp catabolism were the only ones consistently associated with c-IMT/cca-IMT at the cross-sectional visit, as well as cca-IMT progression. Kynurenine and, to a lesser extent, kynurenic acid (KA) have already been identified as correlates with c-IMT and CVD, but these associations were observed mostly in patients with end-stage renal disease [15]. Few studies have evaluated the association between these metabolites and CVD outcomes in HIV-positive individuals. For instance, a study in 105 ART-naïve HIV-positive individuals from Uganda demonstrated that lower absolute values of KTR

6 months after ART initiation, specifically among those achieving an undetectable HIV viral load, were associated with lower c-IMT levels when measured 7 years after treatment initiation [22]. In other cohorts, HIV-positive individuals, compared with HIV-negative, were found to have lower levels of Trp but comparable levels of KA, whereas higher levels of Trp and lower KA or KA/Trp ratio were associated with a decreased risk of carotid artery plaque formation after a median of 7 years of follow-up [23]. Although this study importantly stresses the role of Trp catabolites in increased CVD risk among HIV-positive patients, the relationship with c-IMT was not provided, and other classical Trp catabolites, such as kynurenine, were not measured. Furthermore, this previous observation stemmed from study populations with a high prevalence of comorbidities and smokers, thereby increasing the risk of residual confounding bias.

In our study, we observed that Trp and KA were never identified as metabolite features between HIV/ART groups, yet 5-hydroxy-L-tryptophan was a feature with lower levels in HIV-positive individuals, regardless of ART status. We also confirmed the higher levels of kynurenine in HIV+ ART- individuals compared with HIV-negative individuals [10, 11, 24]. None of these metabolites, however, were associated with c-IMT in our study, and instead only indoleacetate and quinolinate were positively associated with c-IMT after adjusting for age, hypertension, diabetes, and creatinine clearance. Importantly, this association was not apparent in HIV+ ART-naïve and HIV-negative controls, implying that the underlying role of these metabolites in CVD is specific to ART-controlled HIV infection. It should be mentioned that indole-3-acetate and quinolinate have been associated with CVD and/or c-IMT in patients with end-stage renal disease [25, 26]. As all but 2 patients in our cohort had normal creatinine clearance levels, any impact of renal function on our results was likely minimal.

How these metabolite imbalances could consequently impact CVD remains debatable. In a previous study, the KTR largely explained the dysbiosis in gut microbiota observed in HIV+ ART+ vs HIV-negative individuals [27], whereas another study found a close link between Trp or KA levels and several taxa of gut microbiota in HIV-positive individuals [28]. Meanwhile, the KTR has been associated with both altered gut microbiota and endothelial dysfunction in the HIV-positive population [29], suggesting some indirect mechanism associated with intestinal flora. We did observe a strong correlation between KTR and kyurenine levels with sCD14, a marker of active microbial translocation but also innate immune activation [30]. However, their levels were not associated with c-IMT. Systemic inflammation from metabolite imbalances could be another reason for increases in c-IMT, as reported mainly in ART-naïve patients [10]. In our study, kynurenine and KA were strongly associated with D-dimer, whereas quinolinate was only correlated with TNF-α and no other markers of inflammation. Furthermore, there was no correlation between quinolinate or indole-3-acetate and activated or senescent CD4+/CD8+ cells, which could promote systemic inflammatory responses [31]. These observations overall do not support the influence of low-grade inflammation as an explanation for these findings.

Among metabolites of the lysine, carnitine, and dietary choline catabolic pathways, TMAO was not identified as a metabolite feature of HIV+ ART+ compared with HIV- individuals and was not associated with c-IMT [20]. This result is in line with previous findings on coronary artery plaque level [32]. Nevertheless, TMAO might not be an adequate predictor of cardiovascular disease in HIV-positive individuals [20]. We did identify another metabolite from this pathway, g-butyrobetaine, which was negatively associated with c-IMT and cca-IMT. Others have shown the proatherogenic properties of g-butyrobetaine [33], and its levels have already been associated with both carotid artery atherosclerosis and cardiovascular mortality in patients with carotid artery stenosis [13]. However, levels of this metabolite could be reflective of lacking synthesis to carnitine, which leads to TMAO production and further vascular damage [34] or imbalances in gut microbiota [33]. G-butyrobetaine was significantly and positively correlated with naïve T cells, but also senescent CD8+ cells, suggestive of highly active adaptive immune responses in individuals with higher g-butyrobetaine levels. However, the indirect relationship of these metabolites to immunity is unclear. The mechanisms driving the association between g-butyrobetaine and c-IMT require further study in HIV+ ART+ individuals.

Of the metabolites derived from the purine/pyrimidine metabolism pathway, higher xanthosine and uridine levels were associated with higher c-IMT in the present study. Such an association has not been reported previously. Nonetheless, altered levels of metabolites in these pathways, particularly xanthosine and pseudouridine, have been reported in older individuals,

with high expression of genes linked to inflammasome and in turn associated with increased risk of all-cause mortality [35]. A recent study has reported that glutamine levels were increased in matched HIV-positive individuals with vs without coronary artery disease [36], but it only evaluated 15 amino acids. Glutamine levels were decreased in HIV+ ART+ vs HIV+ ART- in our study, yet they were not associated with c-IMT.

Considering the significant differences in metabolite levels between HIV/ART groups observed in our study population and others [8, 24, 37, 38], it is possible that some metabolites are related to the severity of HIV infection [8, 37]. Accordingly, we observed that carnitine from lysine and dietary choline catabolism and xanthine and orotate from the purine/pyrimidine pathway were correlated with nadir CD4+ T-cell count. Higher levels of metabolites from the Trp catabolism pathway were more strongly correlated with lower CD4+ T-cell counts and CD4:CD8 ratio.

HIV infection has been previously associated with mitochondrial dysfunction [8, 37, 38], whereby mitochondrial content within cells increases and results in higher KTR and levels of metabolites from the TCA cycle [38]. Indeed, most metabolites derived from the TCA cycle were identified as metabolite features with higher levels in HIV+ ART- participants, and some were strongly correlated with several inflammatory markers in HIV+ ART+ participants, arguing for mitochondrial dysfunction in the presence of low-grade inflammation during effective ART. Nonetheless, this seemed unrelated to c-IMT.

There are certain limitations of our study. First, the analysis was limited to 48–50 participants in each HIV/ART group. The small sample sizes precluded any in-depth analysis of other factors, such as specific classes of antiretroviral agents. Second, aside from the reduced confounding bias of important factors, namely smoking and gender, due to the exposure-matched design, our results might not be generalizable to other populations. Third, the strict selection of this population likely reduced the variability of metabolite levels, explaining why the criteria for metabolite features included a 0.25-fold $\log_2$ mean change compared with the more commonly used 2-fold change. Nevertheless, the 2-fold cutoff has been criticized as arbitrary and not entirely applicable to metabolomics data [39]. Fourth, there was a significantly higher proportion of HIV+ ART+ individuals with illicit drug use, higher HDL, and lower triglyceride levels than HIV- individuals. These differences could have confounded our findings, yet it is unclear how drug use or lipid parameters influence metabolite concentrations. Finally, analyses of cellular markers of immunity and cca-IMT progression were conducted in a subset of the original study population.

In conclusion, our data suggest that disturbances in the Trp, nucleoside, and Lys-dietary choline catabolic pathways could be involved in HIV-related atherosclerosis. Given that the Trp catabolites TMAO and butyrobetaine are also products of the gut microbiota, an attractive explanation would be that altered

gut microbiota observed in HIV-infected individuals, occurring during ART-induced viral suppression, could contribute to increased risk of atherosclerosis via alterations in the Trp catabolism and lysine and dietary choline degradation pathways. Further research would be needed to confirm this hypothesis.

Supplementary Data

Supplementary materials are available at *Open Forum Infectious Diseases* online. Consisting of data provided by the authors to benefit the reader, the posted materials are not copyedited and are the sole responsibility of the authors, so questions or comments should be addressed to the corresponding author.

References

1. Boccara F, Lang S, Meuleman C, et al. HIV and coronary heart disease: time for a better understanding. J Am Coll Cardiol **2013**; 61:511–23.
2. Kaplan RC, Hanna DB, Kizer JR. Recent insights into cardiovascular disease (CVD) risk among HIV-infected adults. Curr HIV/AIDS Rep **2016**; 13:44–52.
3. Hanna DB, Guo M, Bůžková P, et al. HIV infection and carotid artery intima-media thickness: pooled analyses across 5 cohorts of the NHLBI HIV-CVD collaborative. Clin Infect Dis **2016**; 63:249–56.
4. Desvarieux M, Boccara F, Meynard JL, et al. Infection duration and inflammatory imbalance are associated with atherosclerotic risk in HIV-infected never-smokers independent of antiretroviral therapy. AIDS **2013**; 27:2603–14.
5. Hsue PY, Hunt PW, Sinclair E, et al. Increased carotid intima-media thickness in HIV patients is associated with increased cytomegalovirus-specific T-cell responses. AIDS **2006**; 20:2275–83.
6. Lang S, Mary-Krause M, Cotte L, et al; Clinical Epidemiology Group of the French Hospital Database on HIV. Impact of individual antiretroviral drugs on the risk of myocardial infarction in human immunodeficiency virus-infected patients: a case-control study nested within the French Hospital Database on HIV ANRS cohort CO4. Arch Intern Med **2010**; 170:1228–38.
7. Ryom L, Lundgren JD, El-Sadr W, et al; D:A:D study group. Cardiovascular disease and use of contemporary protease inhibitors: the D:A:D international prospective multicohort study. Lancet HIV **2018**; 5:e291–300.
8. Sitole LJ, Williams AA, Meyer D. Metabonomic analysis of HIV-infected biofluids. Mol Biosyst **2013**; 9:18–28.
9. Peltenburg NC, Schoeman JC, Hou J, et al. Persistent metabolic changes in HIV-infected patients during the first year of combination antiretroviral therapy. Sci Rep **2018**; 8:16947.
10. Jenabian MA, El-Far M, Vyboh K, et al; Montreal Primary infection and Slow Progressor Study Groups. Immunosuppressive tryptophan catabolism and gut mucosal dysfunction following early HIV infection. J Infect Dis **2015**; 212:355–66.
11. Gaardbo JC, Trøseid M, Stiksrud B, et al. Increased tryptophan catabolism is associated with increased frequency of CD161+Tc17/MAIT cells and lower CD4+ T-Cell count in HIV-1 infected patients on cART after 2 years of follow-up. J Acquir Immune Defic Syndr **2015**; 70:228–35.
12. Byakwaga H, Boum Y 2nd, Huang Y, et al. The kynurenine pathway of tryptophan catabolism, CD4+ T-cell recovery, and mortality among HIV-infected Ugandans initiating antiretroviral therapy. J Infect Dis **2014**; 210:383–91.
13. Skagen K, Trøseid M, Ueland T, et al. The carnitine-butyrobetaine-trimethylamine-N-oxide pathway and its association with cardiovascular mortality in patients with carotid atherosclerosis. Atherosclerosis **2016**; 247:64–9.
14. Schiattarella GG, Sannino A, Toscano E, et al. Gut microbe-generated metabolite trimethylamine-N-oxide as cardiovascular risk biomarker: a systematic review and dose-response meta-analysis. Eur Heart J **2017**; 38:2948–56.
15. Wang Q, Liu D, Song P, Zou MH. Tryptophan-kynurenine pathway is dysregulated in inflammation, and immune activation. Front Biosci **2015**; 20:1116–43.
16. Goulenok T, Boyd A, Larsen M, et al; CHIC study group. Increased carotid intima-media thickness is not associated with T-cell activation nor with cytomegalovirus in HIV-infected never-smoker patients. AIDS **2015**; 29:287–93.
17. Aron-Wisnewsky J, Prifti E, Belda E, et al. Major microbiota dysbiosis in severe obesity: fate after bariatric surgery. Gut **2019**; 68:70–82.
18. Garali I, Adanyeguh IM, Ichou F, et al. A strategy for multimodal data integration: application to biomarkers identification in spinocerebellar ataxia. Brief Bioinform **2018**; 19:1356–69.
19. Kanehisa M, Furumichi M, Tanabe M, et al. KEGG: new perspectives on genomes, pathways, diseases and drugs. Nucleic Acids Res **2017**; 45:D353–61.
20. Missailidis C, Neogi U, Stenvinkel P, et al. The microbial metabolite trimethylamine-N-oxide in association with inflammation and microbial dysregulation in three HIV cohorts at various disease stages. AIDS **2018**; 32:1589–98.
21. Shannon P, Markiel A, Ozier O, et al. Cytoscape: a software environment for integrated models of biomolecular interaction networks. Genome Res **2003**; 13:2498–504.
22. Siedner MJ, Kim JH, Nakku RS, et al. Persistent immune activation and carotid atherosclerosis in HIV-infected Ugandans receiving antiretroviral therapy. J Infect Dis **2016**; 213:370–8.
23. Qi Q, Hua S, Clish CB, et al. Plasma tryptophan-kynurenine metabolites are altered in human immunodeficiency virus infection and associated with progression of carotid artery atherosclerosis. Clin Infect Dis **2018**; 67:235–42.
24. Cassol E, Misra V, Holman A, et al. Plasma metabolomics identifies lipid abnormalities linked to markers of inflammation, microbial translocation, and hepatic function in HIV patients receiving protease inhibitors. BMC Infect Dis **2013**; 13:203.
25. Pawlak K, Brzosko S, Mysliwiec M, Pawlak D. Kynurenine, quinolinic acid—the new factors linked to carotid atherosclerosis in patients with end-stage renal disease. Atherosclerosis **2009**; 204:561–6.
26. Dou L, Sallée M, Cerini C, et al. The cardiovascular effect of the uremic solute indole-3 acetic acid. J Am Soc Nephrol **2015**; 26:876–87.
27. Vujkovic-Cvijin I, Dunham RM, Iwai S, et al. Dysbiosis of the gut microbiota is associated with HIV disease progression and tryptophan catabolism. Sci Transl Med **2013**; 5:193ra91.
28. Qi Q, Hua S, Hanna DB, et al. Gut microbiota, tryptophan catabolism and athersclerosis in HIV infection. Paper presented at: Conference on Retroviruses and Opportunistic Infections; February 13–16 **2017**; Seattle, WA. Abstract 636LB.
29. Hoel H, Hove-Skovsgaard M, Hov JR, et al. Impact of HIV and type 2 diabetes on gut microbiota diversity, tryptophan catabolism and endothelial dysfunction. Sci Rep **2018**; 8:6725.

30. Marchetti G, Tincati C, Silvestri G. Microbial translocation in the pathogenesis of HIV infection and AIDS. Clin Microbiol Rev **2013**; 26:2–18.

31. Sauce D, Elbim C, Appay V. Monitoring cellular immune markers in HIV infection: from activation to exhaustion. Curr Opin HIV AIDS **2013**; 8:125–31.

32. Srinivasa S, Fitch KV, Lo J, et al. Plaque burden in HIV-infected patients is associated with serum intestinal microbiota-generated trimethylamine. AIDS **2015**; 29:443–52.

33. Koeth RA, Levison BS, Culley MK, et al. γ-butyrobetaine is a proatherogenic intermediate in gut microbial metabolism of L-carnitine to TMAO. Cell Metab **2014**; 20:799–812.

34. Rydzik AM, Chowdhury R, Kochan GT, et al. Modulating carnitine levels by targeting its biosynthesis pathway - selective inhibition of γ-butyrobetaine hydroxylase. Chem Sci **2014**; 5:1765–71.

35. Furman D, Chang J, Lartigue L, et al. Expression of specific inflammasome gene modules stratifies older individuals into two extreme clinical and immunological states. Nat Med **2017**; 23:174–84.

36. Okeke NL, Craig DM, Muehlbauer MJ, et al. Metabolites predict cardiovascular disease events in persons living with HIV: a pilot case-control study. Metabolomics **2018**; 14:23.

37. Scarpellini B, Zanoni M, Sucupira MC, et al. Plasma metabolomics biosignature according to HIV stage of infection, pace of disease progression, viremia level and immunological response to treatment. PLoS One **2016**; 11:e0161920.

38. Cassol E, Misra V, Mukerji SS, et al. Early markers of renal dysfunction among cocaine users with HIV and HCV infection. Paper presented at: Conference on Retroviruses and Opportunistic Infections; February 22–25 **2016**; Boston, MA. Abstract 693.

39. Vinaixa M, Samino S, Saez I, et al. A guideline to univariate statistical analysis for LC/MS-based untargeted metabolomics-derived data. Metabolites **2012**; 2:775–95.